Tunnel magnetoresistance of C_{60}-Co nanocomposites and spin-dependent transport in organic semiconductors

Shinji Miwa,[1] Masashi Shiraishi,[1,2,*] Shinichi Tanabe,[1] Masaki Mizuguchi,[1] Teruya Shinjo,[1] and Yoshishige Suzuki[1]
[1]*Graduate School of Engineering Science, Osaka University, 1-3 Machikaneyama, Toyonaka, Osaka 560-8531, Japan*
[2]*JST-PRESTO, Kawaguchi, Saitama 332-0012, Japan*

(Received 16 May 2007; revised manuscript received 4 September 2007; published 19 December 2007)

Magnetization, electrical conduction, and magnetoresistance (MR) of C_{60}-Co nanocomposites, where Co nanoparticles are dispersed in C_{60} molecules, have been investigated over a wide temperature range and Co volume fraction. The C_{60}-Co nanocomposites exhibit MR when the Co volume fraction is controlled in such a way that the conduction mechanism is dominated by tunneling of carriers between Co nanoparticles in the C_{60} matrix. The MR, which is attributed to spin-polarized tunneling through the C_{60} molecules, shows strong temperature dependence. Our results indicate that some paramagnetic components contribute to the observed MR. The material-dependent bias-voltage dependence of the MR ratio suggests that these paramagnetic components originate from the interface between organics and ferromagnets. The present study advances the fundamental understanding of spin-dependent transport in organic semiconductors.

DOI: 10.1103/PhysRevB.76.214414 PACS number(s): 75.47.−m, 85.65.+h, 85.75.−d

I. INTRODUCTION

Molecular electronics has been a subject of active research for several decades because of its enormous application potential in organic semiconductors (OSCs), e.g., light-emitting diodes, solar cells, and field-effect transistors. Among various potentials in electronics, rapidly growing attention has been given to molecular spin electronics (spintronics) in the past several years. Because OSCs consist mainly of carbon and hydrogen, they provide longer spin relaxation times than is achievable by conventional spintronics materials, such as metals and inorganic semiconductors. Hence, the introduction of OSCs has led to novel developments in spintronics.

Since the observation of magnetoresistance (MR) in carbon nanotubes with ferromagnetic Co electrodes,[1] injection of spin-polarized carriers into OSCs has been extensively investigated. Spin-dependent transport in OSCs has manifested itself as many investigators reported on MR effects in ferromagnets (FMs)/OSCs/FM junctions.[1–12] Future spin-based devices will most likely involve the injection of spin-polarized carriers into OSCs and the utilization of the long spin lifetime of OSCs. Although room-temperature (RT) MR has been reported in several studies,[7–9,11] MR is typically strongly temperature dependent even in tunnel junctions using OSCs. The mechanism for this temperature dependence remains unclear due to the following reasons. The conduction mechanism has not been determined, especially in spin valves with perpendicular geometry because of the inevitable intermixing of FM and OSCs during sample fabrication.[13] Most experiments in FM/OSCs/FM junctions are not reproducible, and systematic analyses of spin-dependent transport in OSCs have not been implemented to provide insights into underlying physics.

In the present work, we studied electrical and magnetic properties of nanocomposites consisting of ferromagnetic Co nanoparticles dispersed in fullerene (C_{60}) matrix.[3,7,8] C_{60} is one of the most well-investigated OSCs,[14] and has been studied from various perspectives.[15] We previously reported[7] that C_{60}-Co nanocomposites exhibit MR over a wide temperature range (from 4.2 K to RT) as a result of the relative configuration of magnetization in the Co nanoparticles and spin-dependent transport in the C_{60} molecules. Unlike in a previous study,[3] we have improved the material stability by successfully preventing the degradation of C_{60}-Co nanocomposites. Thus, in addition to the transport properties, other important characterizations could be utilized. MR in the C_{60}-Co shows a strong temperature dependence, similar to that in FM/OSCs/FM junctions reported previously.[1–4,7–9,12] The behavior of MR in C_{60}-Co in a wide temperature range and Co volume fraction (expressed as ν_{Co}) reveals that a paramagnetic component may be contributing to the appearance of MR. The resistivity of the paramagnetic component does not saturate under the applied magnetic field (50 kOe). In OSCs-FM nanocomposites, the bias-voltage dependence of the MR ratio depends on the OSC materials; hence, the paramagnetic components are considered to originate from the C_{60}/Co interface. Our study using reproducible devices provides sufficient materials for the discussion of the underlying physics in spin-dependent transport in OSCs.

II. EXPERIMENT

The devices consist of C_{60}-Co nanocomposites sandwiched between nonmagnetic electrodes as schematized in Fig. 1. The preparation process is as follows. First, we fabricate Au electrodes on glass substrates (Corning 1737) with a thickness of 100 nm. Two different types of electrodes, whose gap widths are 37.7 cm (=4.6 mm×82 lines for ν_{Co} =2.5% and 3.9%) and several millimeters (for other samples), are prepared by photolithography and the wire-mask method, respectively. In all devices, the gap length is 100 μm. Then, the C_{60}-Co nanocomposites are prepared by coevaporation under a vacuum of $\sim 4\times10^{-6}$ Pa. The substrate is maintained at 373 K during the coevaporation. C_{60} and Co are deposited by using a resistance-heated alumina crucible and electron-beam evaporator, respectively. The evaporation rate of C_{60} settles at 1.0 Å/s and that of Co

 ©2007 The American Physical Society

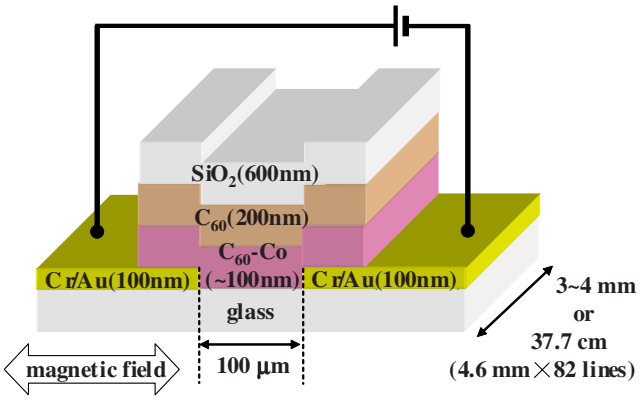

FIG. 1. (Color online) Schematic of a C_{60}-Co nanocomposite device. An in-plane magnetic field (parallel to current) is applied to change the magnetization of each Co nanoparticle in the C_{60}-Co.

depends on the value of ν_{Co}. The value of ν_{Co} is derived from the quartz thickness monitor (Inficon: IC/5). We used Co and C_{60} sources of 99.99% purity. After depositing a buffer layer (C_{60}, 200 nm), a capping layer (SiO_2, 600 nm) is prepared to prevent degradation of the C_{60}-Co nanocomposites. These composites are very sensitive to air, and even tiny pinholes in the capping layer easily induce degradation. Thus, the high-quality capping layer is indispensable; otherwise, resistance of the sample drastically increases upon degradation, giving rise to irreproducibility in the device performance. The SiO_2 layer is deposited by rf magnetron sputtering at a power of 50 W under an Ar pressure of 0.08 Pa. The electrical conduction and MR properties are measured by using a cryostat which contains superconducting solenoids (Oxford, MagLab System[2000]) and a source meter (Keithlay, model 236 source-measure unit). Magnetization measurements are carried out in a superconducting quantum interference device (Quantum Design, MPMS-XL5U).

III. RESULTS

Various structural analyses of C_{60}-Co using transmission electron microscopy (TEM), Raman spectroscopy, and x-ray diffraction (XRD) spectroscopy verified that Co nanoparticles several nanometers in diameter were dispersed in the C_{60} matrix as previously shown.[7]

Magnetizations (M) in the C_{60}-Co nanocomposites as a function of the applied magnetic field (H) measured at 4.2 and 300 K are shown in Figs. 2(a)–2(c). The M-H curves (ν_{Co}=8.2%, 18%, and 27%) at 300 K show no residual magnetization at zero magnetic field and no hysteresis curve, which indicates that the Co nanoparticles in C_{60}-Co show superparamagnetic behavior. On the other hand, the M-H curves at 4.2 K clearly exhibit hysteresis, which is induced by the ferromagnetic properties of the Co nanoparticles. Shown in Fig. 2(d) is the temperature (T) dependence of the magnetizations of C_{60}-Co and a pure Co film measured at H=50 kOe. In C_{60}-Co, the magnetizations decrease with increasing temperature. Figures 2(a)–2(c), reveal that the magnetizations of C_{60}-Co do not saturate even at H=50 kOe, which causes the magnetization in the M-T curve to decrease. Note that zero-temperature magnetizations (obtained by extrapolating the measured values) in the C_{60}-Co are smaller than those of the pure Co film [Fig. 2(d)]. This is presumably because the surface of the Co nanoparticles is chemisorbed with the C_{60} matrix,[16] and thus, lose its magnetic moments, or because the direction of the surface magnetizations is not the same as that of the core in the Co nanoparticles. Figure 2(e) shows the ν_{Co} dependence of average diameters of the Co nanoparticles, which is calculated using a Langevin function from the superparamagnetic behavior at 300 K [Figs. 2(a)–2(c)]. In our previous study,[7] we have verified that the average diameter of the Co nanoparticles in C_{60}-Co deduced from Langevin fitting agreed with the results of TEM and XRD. The diameter decreases with decreasing ν_{Co}, which may be due to the reduction in the evaporation rate of the Co. The decrease in the magnetization almost coincides with the surface areas (portion) of the Co nanoparticles estimated from the Co average diameters [Figs. 2(d) and 2(e)].

The current (I)-voltage (V) characteristics of the C_{60}-Co nanocomposites (ν_{Co}=18%) are shown in Fig. 3(a). It can be noticed that the nonlinear components become significant at high voltage. The nonlinearity, which becomes notable as the temperature decreases, is attributed to the Coulomb energy[17] of the Co nanoparticles in C_{60}-Co. The differential resistance (dV/dI) of C_{60}-Co [Fig. 3(b)] shows that while the current is unstable around 8–14 V, it is stable below and above this voltage range. We attribute this behavior to a change in the carrier conduction path between electrodes. As the voltage is increased above 8–14 V, the current begins to flow through different channels. This behavior does not reflect an irreversible change, such as breakdown of C_{60}-Co, because the I-V characteristics are reproducible. The dV/dI shows discontinuity (~14 V), indicating the existence of a peak in the second derivative of resistance before and after the appearance of the noise. This fact corroborates the above discussion. The temperature dependence of the resistivity (ρ) of the C_{60}-Co nanocomposites is shown in Fig. 3(c). The resistivity is plotted on a logarithmic scale as a function of $T^{-0.5}$. All resistivity values are calculated for a bias voltage of 0.1 V, where the I-V characteristics are linear. The resistivity increases as the temperature decreases, and it can be considered that no percolation path exists in the Co nanoparticles. The ρ values are well fitted by the following equation:

$$\log \rho \propto \left(\frac{T_0}{T}\right)^a, \tag{1}$$

where T_0 is the characteristic temperature and a is a constant. The values of $\log \rho$ are almost proportional to $T^{-0.5}$, and thus, hopping transport,[17] where electrons tunnel between Co nanoparticles, is suggested. Figure 3(d) shows the ν_{Co} dependence of a in Eq. (1). The variation of a will be discussed in the next section.

Figure 4(a) shows the magnetic field dependence of the resistivity of C_{60}-Co nanocomposites (ν_{Co}=18%) for a bias voltage of 0.1 V (solid lines). The MR ratio was found to be 28%. The sweep velocity of the applied magnetic field

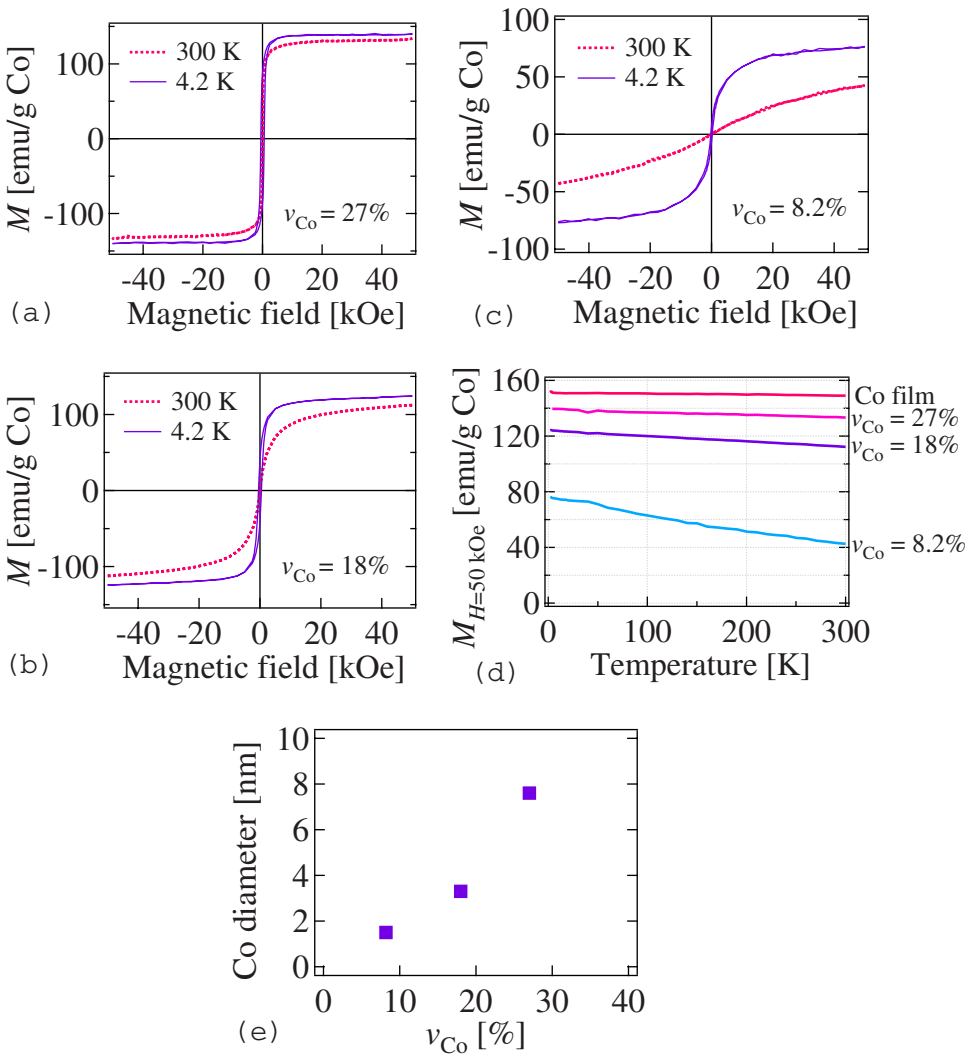

FIG. 2. (Color online) Magnetization in C_{60}-Co nanocomposites. Magnetizations of C_{60}-Co nanocomposites as a function of applied magnetic field at 4.2 and 300 K for devices with different Co volume fractions: v_{Co}=27% (a), 18% (b), and 8.2% (c). (d) Temperature dependence of M in C_{60}-Co and a pure Co film measured at H=50 kOe. (e) Average diameters of Co nanoparticles in C_{60}-Co. The values are calculated from the superparamagnetic behavior at 300 K.

was about 0.1 kOe/s. Here, MR ratio is defined as $(\rho_{max}-\rho_{min})/\rho_{min}$, where ρ_{max} and ρ_{min} are the maximum and minimum resistivities, respectively. A negative MR is commonly observed in the composites of ferromagnetic nanoparticles and nonmagnetic matrices.[18,19] Figure 4(a) also shows the square of the normalized magnetization $-(M/M_s)^2$ (open circles), where M is the global magnetization and M_s is the saturation magnetization. This curve almost corresponds to the ρ-H curve,[19] which suggests that the MR is induced by spin-dependent transport in the C_{60} molecules. As reported in our previous study,[7] good agreement is seen between the values of ρ and $-(M/M_s)^2$ at RT, while deviation is seen for high magnetic fields at low temperature (4.2 K). Compared to the magnetization, the MR ratio does not saturate even at H=50 kOe. We believe that the size distribution of Co nanoparticles is playing a role in this behavior. In addition, the surface magnetization behavior may not be synchronized with that of the cores in the Co nanoparticles.

Figure 4(b) shows the temperature dependence of the MR ratio of C_{60}-Co nanocomposites for a bias voltage of 0.1 V. Samples with low v_{Co} (2.5%, 3.9% and 7.2%) did not exhibit any MR (less than ~0.1%) over the investigated temperature range (4.2–300 K). In nanocomposite systems, the MR ratio can be expressed by the following equation based on the Julliere model:[20,21]

$$\text{MR ratio} = P^2, \tag{2}$$

where P is the spin polarization of the ferromagnets. When P is taken to be 34%,[22] the calculated MR ratio is about 12%. We have obtained MR ratios larger than the calculated value (12%) at liquid helium temperature [Fig. 4(b)]. However, most of the samples exhibit a monotonous decrease in MR ratio with increasing temperature, reaching a value less than 1% at RT. The temperature dependence is well described by a power law:

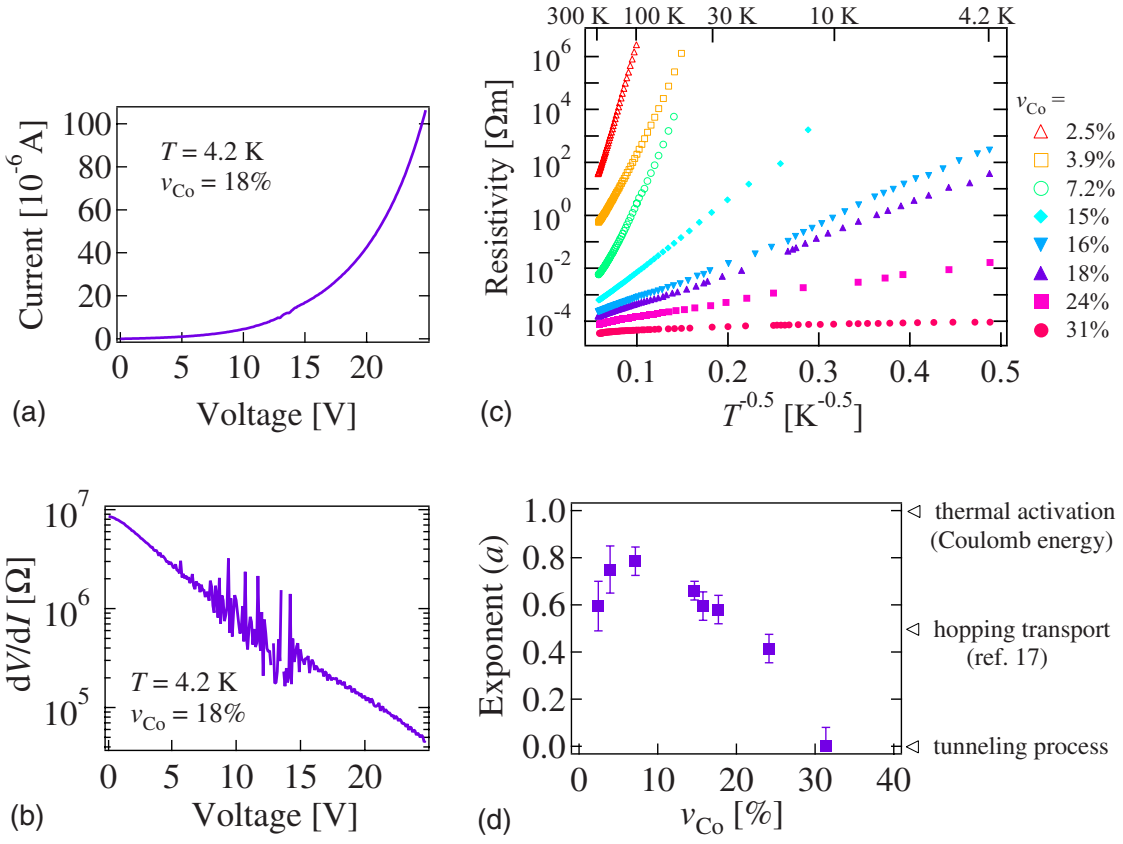

FIG. 3. (Color online) Electrical properties in C_{60}-Co nanocomposites. (a) I-V characteristics of C_{60}-Co nanocomposites (ν_{Co}=18%) at 4.2 K. (b) Differential resistance (dV/dI) of C_{60}-Co. The value of dV/dI is calculated from the I-V curve. (c) Temperature dependence of zero-bias resistivities in log $\rho - T^{-0.5}$ plot. (d) The Co volume fraction (ν_{Co}) dependence of a when log ρ is described as $(T_0/T)^a$. The value of a is obtained by a least-square method.

$$\text{MR ratio} \propto T^{-b}, \tag{3}$$

where b is an exponent determined by the least-square method. Figure 4(c) shows the ν_{Co} dependence of b.

We also examined the MR of a sample without Co nanoparticles (ν_{Co}=0%), which yielded a very small (~0.04% at 300 K) positive MR. The MR originates from the C_{60}'s themselves. The dependence of MR ratio on applied magnetic field, temperature, and bias voltage resemble that of other OSCs.[23] Positive MR values were also observed (MR ratio ~0.03% at 4.2 K) in the case of a metallic C_{60}-Co (ν_{Co}=46%), for which the resistance decreased with decreasing temperature. This indicates the absence of C_{60}'s in the carrier conduction paths between the electrodes. The phenomenon can thus be attributed to anisotropic MR of percolating Co nanoparticles. It should be noted that these two instances of positive MR are immediately distinguishable from that of the spin-polarized tunneling between Co nanoparticles via C_{60} molecules because the sign of the MR is different.

The bias-voltage dependence of the MR ratio in the C_{60}-Co nanocomposites (ν_{Co}=18%) at 4.2 K is shown in Fig. 4(d). Two important features are observed. First, the MR ratio decreases as the voltage increases from 0 to ~8 V, which is typical for magnetic tunnel junctions (MTJs).[24] Second, the MR ratio is enhanced between 8 and 14 V. Previous studies[7,8] reported a similar enhancement. However, in our study, the MR-V curve shows a peak, which was not observed in the Co/Co-C_{60} systems studied by Sakai *et al.*,[8] where the MR ratio was observed to increase monotonically. It can be noticed that the voltage range of 8–14 V, where the MR-V curve exhibits a peak, corresponds to that where noise appears in the differential resistance [Fig. 3(b)]. We may expect a monotonic increase if the current flows in the same path in the C_{60}-Co nanocomposites for all bias voltages. While the behaviors of the MR at low bias voltage (magnitude of the MR ratio, temperature dependence, and so on) are very similar with those reported in Ref. 8, behaviors at high bias voltages are different. This discrepancy is presumably due to differences in sample fabrication.[25]

IV. DISCUSSION

The conductance of C_{60}-Co nanocomposites is determined by optimizing the tunneling probability and the Coulomb energy of the Co nanoparticles.[17] This yields 0.5 as the value of a in Eq. (1), which is typical for insulating granular systems.[26] However, evaluation of a using the least-square method results in a distribution [Fig. 3(d)]. The dependence of a on ν_{Co} can be summarized as follows. For ~15% $< \nu_{Co} <$ ~25%, a is approximately 0.5, and the conduction is precisely explained by the model mentioned above.[17]

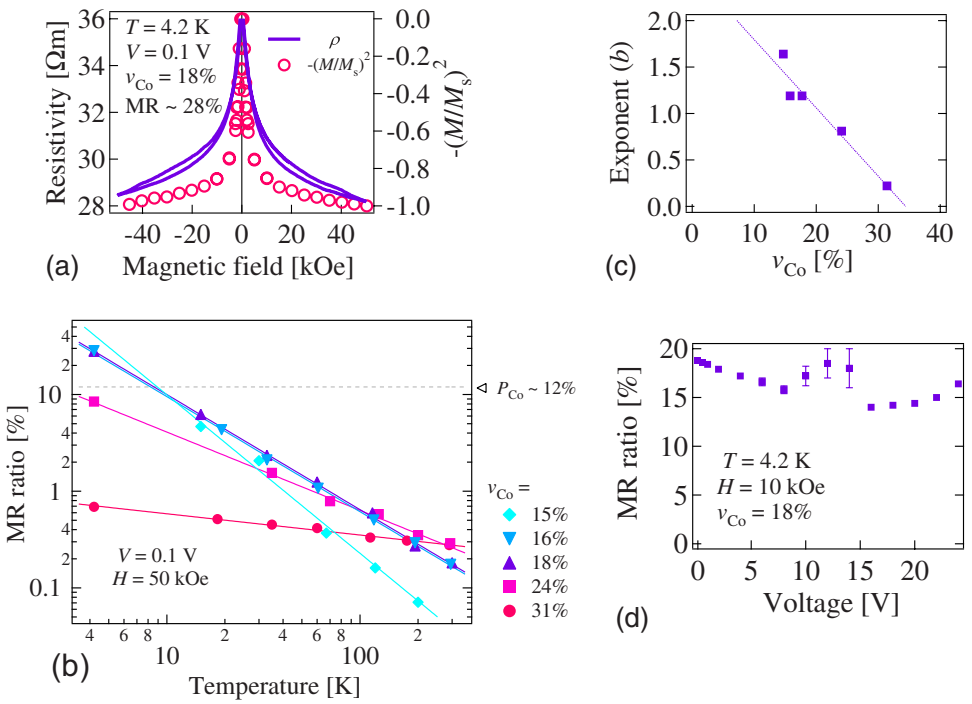

FIG. 4. (Color online) Magnetoresistance in C_{60}-Co nano-composites. (a) Electrical resistivity of C_{60}-Co nanocomposites ($\nu_{Co}=18\%$) as a function of applied magnetic field at 4.2 K for a bias voltage of 0.1 V (solid lines). The relationship between ρ and $-(M/M_s)^2$ is shown (open circles). (b) Temperature dependence of the MR ratio in C_{60}-Co nanocomposites. Solid lines are power-law fits obtained by a least-square method. The dashed line represents the MR value of P_{Co}^2 expected from spin polarization of Co, $P_{Co}=34\%$ (Ref. 22). (c) Co volume fraction (ν_{Co}) dependence on fitting parameter b. The dotted line is a fit using a least-square method. (d) Bias-voltage dependence of the MR ratio in the C_{60}-Co ($\nu_{Co}=18\%$) measured at 4.2 K.

When the Co volume fraction exceeds ~25%, a is nearly zero, which is a characteristic of tunneling conduction without charging effects (temperature independent, $a=0$). The value of a is strongly affected by the Coulomb energy for small ν_{Co} ($\sim 7\% < \nu_{Co} < \sim 15\%$), where a is close to 1. The behavior of a in this range of ν_{Co} is consistent with the size of the nanoparticles [Fig. 2(e)] because the Coulomb energy of Co nanoparticles varies inversely with particle size. For lower values of ν_{Co} ($< \sim 7\%$), a decreases with decreasing ν_{Co} (less than ~7%) because Co nanoparticles are no longer present in C_{60} matrices and do not contribute to the carrier conduction.[27] The threshold value of ~7% agrees with the value of ν_{Co} volume where the Co nanoparticles start to form in the C_{60} molecules, as reported in the literature.[16] The above discussion leads us to conclude that tunneling between Co nanoparticles is the dominant conduction mechanism in the C_{60}-Co nanocomposites with Co volume fractions in the range of $\sim 7\% < \nu_{Co} < \sim 35\%$, where the MR effect is observed.

We now focus our discussion on the temperature dependence of MR of the C_{60}-Co nanocomposites [Fig. 4(b)]. We assume that the strong temperature dependence is not the result of the loss of magnetization in the Co bulk or surface because the ferromagnetic transition temperature of Co (T_c =1388 K) is well above the temperature range examined in this study. One of the possible explanations is the enhancement of MR by Coulomb blockade.[26,28] As discussed above, the Coulomb energy of the Co nanoparticle influences the electrical conduction. It is, therefore, likely that the temperature dependence of MR is induced by the cotunneling process. However, the effects of Coulomb blockade are expected to be dominant only at low temperature (below several tens of kelvins),[26] whereas the observed temperature dependence of MR continues for higher temperature. It should, therefore, be noted that there are other factors influencing the temperature dependence of MR in addition to Coulomb blockade.[26,28]

The temperature dependence of MR in C_{60}-Co is distinctly different from that of inorganic MTJs,[24,29] which is typically weakly temperature dependent. It is widely recognized that MR of inorganic multilayered MTJs[24,29] as well as of insulating granular systems[26,30] can be well described by the Julliere model.[20] The fact that MR ratio does not decrease with increasing temperature when the magnetic moments saturate leads us to conclude that some paramagnetic components that do not saturate at $H=50$ kOe govern MR in C_{60}-Co nanocomposites. One possible cause is the appearance of scattering centers in the C_{60}'s. In the C_{60}-Co nanocomposites, C_{60} molecules act as tunnel barriers, and the carriers directly tunnel between the Co nanoparticles. It is known that impurity-doped barriers lower the MR ratio in MTJs;[31] however, the temperature dependence of MR is clearly different from that of C_{60}-Co nanocomposites. Based on these considerations, we now discuss the appearance of MR by taking into account a paramagnetic component, which is a source of spin-polarized carriers. The disappearance of magnetization [Fig. 2(d)] and slowly saturating ρ-H curve [Fig. 4(a)] corroborate the existence of the paramagnetic component. This component may arise from (1) super-

paramagnetism of Co nanoparticles and/or (2) C_{60}/Co interface states. In the former case, suppression of MR results due to the presence of Co nanoparticles with small diameters (much less than the average diameter of several nanometers) that contain unsaturated magnetization. Such small particles can be introduced during the evaporation. In the latter case, the C_{60}/Co interface may have different states from that of pure Co and contribute to the appearance of the MR. The formation of a C_{60}-Co_x complex has previously been reported,[16] and the influence of the complex on the temperature dependence of MR has been mentioned.[8] The influence of the paramagnetic components is thought to increase with decreasing ν_{Co} because small ν_{Co} results in C_{60}-Co nanoparticles with small diameter, thereby increasing the total surface area of the Co nanoparticles.

On the basis of the above-mentioned model, the observed temperature dependence of the MR ratio can be explained as follows. For large ν_{Co}, the influence of the paramagnetic components is presumably small, and the MR effect is almost exclusively governed by ferromagnetic components, i.e., the magnetization in the Co nanoparticles. MR ratio is thus temperature independent for sufficiently large ν_{Co}:

$$\text{MR ratio} = \text{const.} \quad (\nu_{Co} \rightarrow \text{large}). \tag{4}$$

On the other hand, for smaller ν_{Co}, the paramagnetic component becomes dominant. In general, the *M-H* curve of paramagnetic moments is approximately described by the Langevin function, and the high-temperature expansion of the function is inversely proportional to *T*. Using Eq. (2), the temperature dependence of the MR ratio can be expressed as

$$\text{MR ratio} \propto \frac{1}{T^2} \quad (\nu_{Co} \rightarrow \text{small}). \tag{5}$$

In Fig. 4(c), extrapolating the fitting curve to $b=0$ yields $\nu_{Co} \sim 34.6\%$, which is considered to be the percolation limit. On the other hand, at the limit of small ν_{Co} ($<10\%$), *b* exceeds 2 in the fitting curve even though $b=2$ has to be the maximum according to Eq. (5). For $b=2$, ν_{Co} is $\sim 7.3\%$, which is the volume fraction where hopping starts to govern the transport mechanism as discussed above. This value also corresponds to the threshold for the formation of Co nanoparticles.[16] Thus, the description above can explain the experimental data very well. A mixture of the ferromagnetic component, which is commonly observed in inorganic insulating granular systems like Co-Al-O,[26] and a paramagnetic component can explain the observed MR in the C_{60}-Co nanocomposites.

Bias-voltage dependence of MR in C_{60}-Co nanocomposites is unique as compared to that in typical inorganic MTJs.[24,29] We have previously investigated[32,33] a series of nanocomposites of Co nanoparticles and OSC matrices, such as tris 8-hydroxyquinoline aluminum ($C_{27}H_{18}AlN_3O_3$, Alq_3) and 5,6,11,12-tetraphenylnaphthacene ($C_{42}H_{28}$, rubrene), which are known as typical OSCs in molecular electronics. Alq_3-Co and rubrene-Co nanocomposites exhibit magnetization, electrical conduction, and magnetoresistance that highly resemble those in C_{60}-Co; however, MR-*V* characteristics are notably different. Figure 5 shows a comparison of the MR-*V* curves for C_{60}-Co ($\nu_{Co}=18\%$) and for Alq_3-Co ($\nu_{Co}=29\%$) measured at 4.2 K. Coulomb energy (E_C) of the Co nanoparticles in the Alq_3-Co is estimated[17] (from ρ-*T* curves) to be 3.29 meV, which is larger than the value estimated for C_{60}-Co ($E_C=2.55$ meV). This is possibly the result of charging effects in Alq_3-Co ($\nu_{Co}=29\%$) being larger than those in C_{60}-Co ($\nu_{Co}=18\%$). While the increase of the MR ratio ($\sim 8 < V < \sim 14$ V) in C_{60}-Co can be attributed to the Coulomb blockade in the Co nanoparticles,[26,28] such trends are not seen for either Alq_3-Co or rubrene-Co systems. If the influence of the Coulomb blockade were dominant in the MR-*V* curve for the C_{60}-Co system, the same trends should be expected for the Alq_3-Co and rubrene-Co systems. Therefore, it is natural to think that the anomalous bias-voltage dependence of MR in C_{60}-Co nanocomposites results from C_{60}/Co interface states. The variability observed in different matrix materials suggests that the OSC/FM interface has different interface states depending on OSC species. The paramagnetic moments, which have significant influence on the MR, are believed to be due to the C_{60}/Co interface.

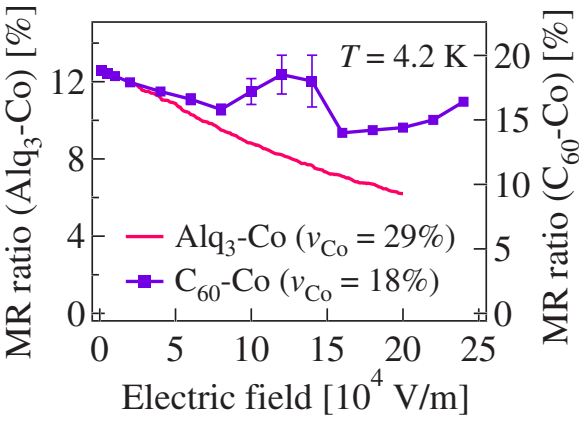

FIG. 5. (Color online) A comparison of applied bias-voltage dependence of MR ratio in C_{60}-Co and Alq_3-Co (Ref. 32) nanocomposites measured at 4.2 K.

V. CONCLUSION

We have examined various properties of C_{60}-Co nanocomposites. Magnetization, electrical conduction, and MR measurements reveal that spin-polarized carriers tunnel between Co nanoparticles through C_{60} molecules. The MR exhibits strong temperature dependence, which is commonly observed in FM/OSCs/FM junctions. While the temperature dependence of FM/OSCs/FM junctions is typically attributed to the disappearance of magnetization in FM or spin scattering in OSCs, its mechanism has not been understood. We have provided sufficient materials for theoreticians to implement quantitative analyses of the temperature dependence of MR in FM/OSCs/FM junctions, and one can discuss the underlying physics of the spin-dependent transport in OSCs. The observed temperature dependence in C_{60}-Co nanocomposites cannot be explained only by the Coulomb blockade effect in Co nanoparticles,[26,28] and the results of this study shed light on factors with the following features: a large

saturation field and significant influence on MR. For further research in molecular spintronics, such paramagnetic components require careful consideration in understanding the intrinsic effects of the materials. If the component originates from FM/OSCs interfaces, interface control, for example, by inserting a high-quality insulating layer, such as alumina, into OSCs/FM interfaces, may improve efficient spin injection into OSCs even at room temperature.

ACKNOWLEDGMENTS

We would like to thank the Low Temperature Center at Osaka University and S. Morimoto for their help with magnetization measurements. The assistance of S. Nishioka and H. Tomita was greatly appreciated. This research has been supported by the New Energy and Industrial Technology Development Organization (NEDO).

*Corresponding author; shiraishi@mp.es.osaka-u.ac.jp

[1] K. Tsukagoshi, B. W. Alphenaar, and H. Ago, Nature (London) **401**, 572 (1999).
[2] Z. H. Xiong, D. Wu, Z. V. Vardeny, and J. Shi, Nature (London) **427**, 821 (2004).
[3] H. Zare-Kolsaraki and H. Micklitz, Eur. Phys. J. B **40**, 103 (2004).
[4] J. R. Petta, S. K. Slater, and D. C. Ralph, Phys. Rev. Lett. **93**, 136601 (2004).
[5] S. Sahoo, T. Kontos, J. Furer, C. Hoffmann, M. Gräber, A. Cottet, and C. Schönenberger, Nat. Phys. **1**, 99 (2005).
[6] N. Tombros, S. J. van der Molen, and B. J. van Wees, Phys. Rev. B **73**, 233403 (2006).
[7] S. Miwa, M. Shiraishi, M. Mizuguchi, T. Shinjo, and Y. Suzuki, Jpn. J. Appl. Phys., Part 2 **45**, L717 (2006).
[8] S. Sakai, K. Yakushiji, S. Mitani, K. Takanashi, H. Naramoto, P. V. Avramov, K. Narumi, V. Lavrentiev, and Y. Maeda, Appl. Phys. Lett. **89**, 113118 (2006).
[9] S. Majumdar, R. Laiho, P. Laukkanen, I. J. Väyrynen, H. S. Majumdar, and R. Österbacka, Appl. Phys. Lett. **89**, 122114 (2006).
[10] S. Pramanik, S. Bandyopadhyay, K. Garre, and M. Cahay, Phys. Rev. B **74**, 235329 (2006).
[11] T. S. Santos, J. S. Lee, P. Migdal, I. C. Lekshmi, B. Satpati, and J. S. Moodera, Phys. Rev. Lett. **98**, 016601 (2007).
[12] L. E. Hueso, J. M. Pruneda, V. Ferrari, G. Burnell, J. P. V. Herrera, B. D. Simons, P. B. Littlewood, E. Artacho, A. Fert, and N. D. Mathur, Nature (London) **445**, 410 (2007).
[13] A. C. Dürr, F. Schreiber, M. Kelsch, H. D. Carstanjen, and H. Dosch, Adv. Mater. (Weinheim, Ger.) **14**, 961 (2002).
[14] R. C. Haddon, A. S. Perel, R. C. Morris, T. T. M. Palstra, A. F. Hebard, and R. M. Fleming, Appl. Phys. Lett. **67**, 121 (1995).
[15] M. S. Dresselhaus, G. Dresselhaus, and P. S. Eklund, *Science of Fullerenes and Carbon Nanotubes* (Academic, New York, 1996).
[16] S. Sakai, H. Naramoto, Y. Xu, T. H. Priyanto, V. Lavrentiev, and K. Narumi, MRS Symposia Proceedings No. 788 (Materials Research Society, Pittsburgh, 2004), p. L11.49.
[17] P. Sheng, B. Abeles, and Y. Arie, Phys. Rev. Lett. **31**, 44 (1973).
[18] A. E. Berkowitz, J. R. Mitchell, M. J. Carey, A. P. Young, S. Zhang, F. E. Spada, F. T. Parker, A. Hutten, and G. Thomas, Phys. Rev. Lett. **68**, 3745 (1992).
[19] J. Q. Xiao, J. S. Jiang, and C. L. Chien, Phys. Rev. Lett. **68**, 3749 (1992).
[20] M. Julliere, Phys. Lett. **54A**, 225 (1975).
[21] In the Julliere model, conductance (σ) is proportional to $1+P^2\cos\theta$, where P is a spin polarization of ferromagnets. The MR ratio is described as $(\rho_{\max}-\rho_{\min})/\rho_{\min}=(\sigma_{\min}^{-1}-\sigma_{\max}^{-1})/\sigma_{\max}^{-1}=[(1+P^2)-1]/1=P^2$. The value of θ varies between 0 and $\pi/2$ in the nanocomposites, while between 0 and π in the multilayered spin valve.
[22] P. M. Tedrow and R. Meservey, Phys. Rev. B **7**, 318 (1973).
[23] Ö. Mermer, G. Veeraraghavan, T. L. Francis, Y. Sheng, D. T. Nguyen, M. Wohlgenannt, A. Köhler, M. K. Al-Suti, and M. S. Khan, Phys. Rev. B **72**, 205202 (2005).
[24] J. S. Moodera, L. R. Kinder, T. M. Wong, and R. Meservey, Phys. Rev. Lett. **74**, 3273 (1995).
[25] As far as we know, the fabrication processes of samples are slightly different. For instance, the substrate temperatures during evaporation are 373 and 473 K in our and the other group's studies, respectively. The other group employs step-by-step evaporation instead of coevaporation method used in this study. The electrode materials and the sample sizes are also different. However, apparently, there is no major difference in the sample fabrication process. The degree of vacuum during evaporation of C_{60} and Co is good enough in both, but, unfortunately, we do not have precise information about the quality of capping layers employed in Ref. 8 We believe that the capping layers are critical for preventing the degradation of samples and allow us to obtain reliable data, and the result and discussion in this study are essential and universal in C_{60}-Co systems.
[26] S. Mitani, S. Takahashi, K. Takanashi, K. Yakushiji, S. Maekawa, and H. Fujimori, Phys. Rev. Lett. **81**, 2799 (1998).
[27] N. F. Mott, Philos. Mag. **19**, 835 (1969).
[28] S. Takahashi and S. Maekawa, Phys. Rev. Lett. **80**, 1758 (1998).
[29] T. Miyazaki and N. Tezuka, J. Magn. Magn. Mater. **139**, L231 (1995).
[30] J. Inoue and S. Maekawa, Phys. Rev. B **53**, R11927 (1996).
[31] R. Jansen and J. S. Moodera, Phys. Rev. B **61**, 9047 (2000).
[32] S. Tanabe, S. Miwa, M. Mizuguchi, T. Shinjo, Y. Suzuki, and M. Shiraishi, Appl. Phys. Lett. **91**, 063123 (2007).
[33] H. Kusai, S. Miwa, M. Mizuguchi, T. Shinjo, Y. Suzuki, and M. Shiraishi, Chem. Phys. Lett. **448**, 106 (2007).